JOURNAL OF SOLID STATE CHEMISTRY 103, 176–185 (1993)

Hexagonal and Pyrochlore-Type Cesium Tungstate Synthesized from Cesium Peroxo-Polytungstate and Their Redox Chemistry

JUNKO OI, AKIRA KISHIMOTO, AND TETSUICHI KUDO[1]

Institute of Industrial Science, University of Tokyo, 7-22-1, Roppongi, Minato-ku, Tokyo 106, Japan

Received May 27, 1992; in revised form August 17, 1992; accepted August 20, 1992

Thermal decomposition of cesium peroxo-polytungstate, an amorphous precursor, yielded not only pyrochlore-type but also hexagonal WO_3-type cesium tungstate, depending on the Cs/W ratio (x) in the precursors; the former is in the range $0.48 \leq x \leq 0.54$ and the latter $0.30 \leq x \leq 0.34$. Mixtures of these two phases were formed in the intermediate region of x. On reduction at 700°C, the pyrochlore phase gave a compound with the same framework, with its cubic cell parameter being elongated from 10.25 to 10.32 Å, but reoxidation resulted in a mixture of pyrochlore and hexagonal phases. In contrast, reduction and oxidation of the hexagonal phase at 600°C was reversible. Powder XRD profile refinements were performed with reduced and oxidized hexagonal cesium tungstates ($x = 0.30$) in the space group $P6_3/mcm$. The former compounds ($a = 7.4049(1)$ and $c = 7.6098(1)$) are based on an almost idealized h-WO_3 framework with Cs sitting on its large $2b$ interstices ($R_I = 0.0240$). The oxidized compounds (7.4012(18) and 7.6728(17)Å, $R_I = 0.007$) possessed a lacunar tungsten sublattice.

Introduction

Tungsten- or molybdenum-based compounds with the framework structures attract much attention in relation to intercalation chemistry, which provides the basis for many applications, including secondary batteries, etc. In this connection, synthetic routes for pyrochlore- or hexagonal-tungstates, the common frameworks of which are built out of six-membered rings of corner-sharing WO_6 octahedra, have extensively been investigated.

We have reported defective pyrochlore-type $xCsO_{0.5} \cdot WO_3$ (or more properly $Cs_yW_{1-y/6}O_3$, where $y = 6x/(6 + x)$) synthesized by thermal decomposition of an amorphous salt precipitated by reacting peroxo-polytungstic acid with CsCl solution (*1*, *2*). Previously, Coucou and Figlarz had succeeded in synthesizing similar tungstates in an acidic ethylene glycol solution (*3*). Very recently, Driouiche *et al.* prepared the same class of compound by reacting h-WO_3 and Cs_2CO_3 in the solid state at 300°C (*4*). Common features of these syntheses are that the reaction temperatures are relatively low and the products are in a fully oxidized state in which their tungsten sublattice is defective.

On the other hand, hexagonal tungstates incorporated with large cations such as Cs^+ or Rb^+ have not yet been synthesized by the low-temperature process, though we have reported that $xKO_{0.5} \cdot WO_3$ in a hexagonal form is successfully obtained from po-

[1] To whom correspondence should be addressed.

0022-4596/93 $5.00

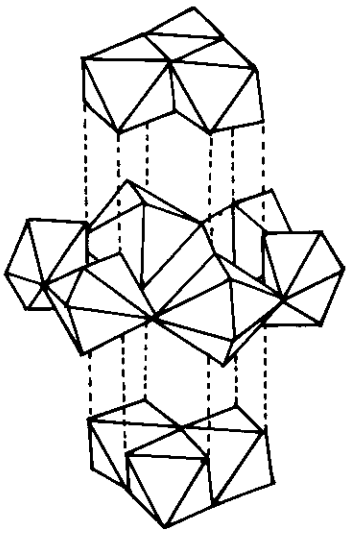

FIG. 1. Structural model of IPA (peroxo-polytungstic acid) anion.

tassium peroxopolytungstate (*2*), and Reis *et al.* obtained its sodium version using a hydrothermal technique (*5*). To date, however, Cs- or Rb-tungstate with such a framework can only be synthesized as a reduced state by the conventional Magneli's method (*6*) in which a mixture of Cs_2WO_4 and WO_2 (or Cs_2WO_4, WO_3, and W) is reacted under vacuum at high temperature.

In this paper we report the synthesis of hexagonal Cs-tungstate via peroxo-polytungstic acid and its structural aspects. Redox chemistry of hexagonal- and pyrochlore-type Cs-tungstate is also described.

Synthetic Procedure

Peroxo-polytungstic acid (starting material, denoted as "IPA") was prepared according to the previously reported method (*7*). In short, metallic W powder was dissolved in 15% H_2O_2 to yield a pale yellow acidic solution. It was then dried at room temperature after removing excess H_2O_2 catalytically with a platinized Pt net, resulting in a yellow glassy substance (= IPA) with an approximate empirical formula of $2WO_3 \cdot H_2O_2 \cdot 2H_2O$. The whole structure of IPA is not thoroughly understood because of its noncrystalline nature. However, it was found by our recent XRD analysis (*8*) that the observed radial distribution function of IPA agreed very well with the calculated one from a polyanion model shown in Fig. 1, which was also consistent with its vibrational spectra. Thus this model is the most probable picture of the IPA-polyanion to date.

Cesium peroxo-polytungstate (white amorphous substance, denoted as "Cs-IPA") was precipitated by adding 10 ml of IPA solution (containing 7.0 mmol of W) into 20 ml of stirred CsBr solution with a concentration ranging from 0.12 to 1.41 mol · liter^{-1}. During this process, part of peroxides in the polyanion were reduced and a significant amount of Br_2 was isolated. After overnight storage, the precipitate was filtrated, rinsed with water, and dried at 80°C. The X-ray fluorescence analysis showed that the Cs/W ratios (x) in Cs-IPA thus obtained varied from 0.30 to 0.59, as shown in Table I, depending on the initial mixing ratios. However, every Cs-IPA in Table I may be constructed out of IPA or its condensed polyanions, because their IR spectra are almost identical to that of IPA itself, as shown in Fig. 2.

The TG and DTA results (Fig. 3), re-

TABLE I

Cs/W RATIOS IN INITIAL MIXTURE AND Cs-IPA

Mixing Cs/W ratio	0.5	1	2	3	6
Cs/W in precipitate (= Cs-IPA)	0.30	0.40	0.48	0.54	0.59

Note. [W^{6+}] = 0.23 mole · liter^{-1} (= constant).

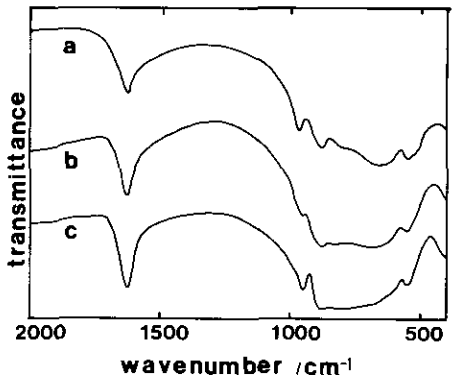

FIG. 2. IR spectra of IPA and as-prepared Cs-IPA. (a) IPA, (b) Cs-IPA (Cs/W = 0.30) and (c) Cs-IPA (Cs/W = 0.48).

corded for a Cs-IPA (x = 0.30) in air, showed that it decomposes simply one-stepwise and starts crystallizing near 350°C. Cs-IPAs in other compositions decompose in the same way, but, as shown in Fig. 4, the peak temperature of the crystallization heat is lowered from 390°C (for x = 0.3) to 350°C (x = 0.59) and the peak is remarkably sharpened as x is increased. Powder X-ray diffraction (Fig. 5) showed that the products after crystallization, which were white to pale-yellow matter, took a HTB (hexagonal tungsten bronze)-type structure for x = 0.30 ~ 0.34 and a pyrochlore-type for 0.48 ~ 0.59.

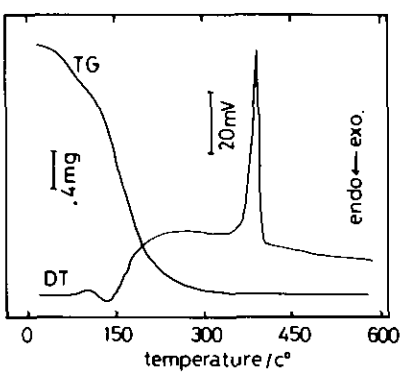

FIG. 3. TG/DT spectra of Cs-IPA (Cs/W = 0.30).

But an intermediate composition (x = 0.4, for example) gave a mixture of these two phases.

Both phases thus formed were stable up to about 700°C and then gradually disproportionated into unknown phases. It is noted that this is the first synthesis of fully oxidized hexagonal cesium tungstate.

On heating Cs-IPA (x = 0.30) in a reducing atmosphere (10% H_2/0.5% H_2O/N_2-balance) instead of air at 600°C, dark blue hexagonal Cs-tungstate was obtained. This reduced compound had very high crystallinity, as shown in XRD pattern Fig. 6a. However, Cs-rich precursors (x = 0.48 or more) yielded a mixture of hexagonal and pyrochlore phase under the same synthetic conditions, as shown in Fig. 6b. We found that this mixture turned into an almost single pyrochlore phase with high crystallinity in a reducing atmosphere (H_2/H_2O) as the reaction temperature was raised up to 700°C, as shown in Fig. 6c. A very weak peak at 2θ = 40° was probably due to metallic W.

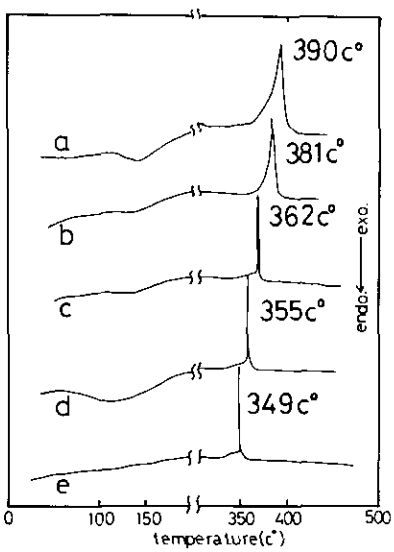

FIG. 4. DT spectra of Cs-IPA with various Cs/W ratios. Atmosphere, air, heating rate, 25°C min^{-1}. (a) Cs/W = 0.30, (b) 0.40 (c) 0.48 (d) 0.54 and (e) 0.59.

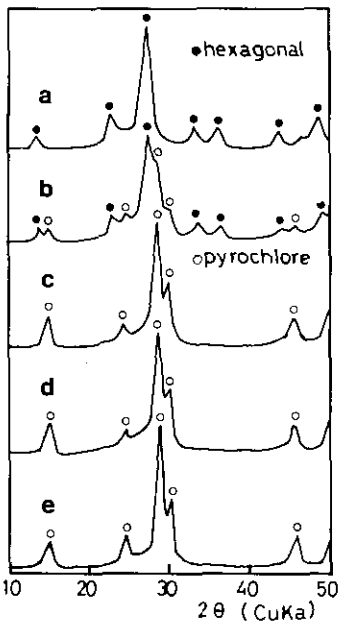

FIG. 5. XRD of Cs-tungstates synthesized from amorphous Cs-IPA with various Cs/W ratios. Heat-treatment conditions; in air at 600°C for 1 h. (a) Cs/W = 0.30, (b) 0.40, (c) 0.48, (d) 0.54,and (e) 0.59.

Structural Analysis

Powder XRD profile refinements were performed for the present hexagonal Cs-tungstates on the Rietveld method using the RIETAN computational system (*9*). Samples in an oxidized and reduced form were prepared by heating Cs-IPA ($x = 0.30$) at 600°C for 1 h in air and in a reducing atmosphere (10% H_2/0.5% H_2O/N_2-balance), respectively. Crystallographic data were collected with an X-ray powder diffractometer using monochromatized Cu*K*a radiation. The 2θ-scanning was stepwise with the width of 0.026° and the measuring time was 4 sec. To diminish orientation effects, the sample was well ground and attached as lightly as possible on a sample holder.

Systematic absences of reflections 001 and h0*l* ($l \neq 2n$) were clearly found in the highly resolved pattern taken with the reduced sample in the range $5° \leq 2\theta \leq 115°$. We thus selected the space group $P6_3/mcm$, in which the structure of various HTBs had been solved (*10–12*). Tungsten and oxygen were distributed at 6*g*, 12*k* (for O(1)), and 12*j* (for O(2)) according to Labbe's positioning for Rb-HTB (12). The occupancy of each site was fixed at 1.0, 0.5, and 1.0, respectively, because, spectroscopic and density data (shown later) suggested that reduced Cs-tungstate represented by Cs_xWO_3 ($z = 6$) have a complete h$-WO_3$-type framework. The Cs position was fixed at 2*b* (the origin) with the occupancy being 3*x*(0.90 for this case according to the analytical result). It was found that locating it at other sites (2*a* or the more general 4*e* position) only led to poorer convergence. Thus, the refined atomic parameters were five, W and O coordinate parameters and B-values of the composition ions. The observed and calculated pattern are compared in Fig. 7a.

The final results of the refinement (R_f = 0.024) for reduced h-Cs_xWO_3 (x = 0.30) are shown in Table IIa, indicating that a h-WO_3-type framework of the compound takes al-

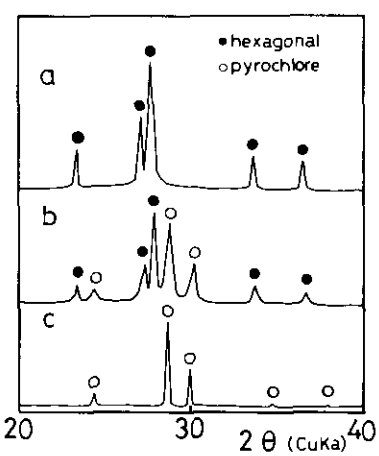

FIG. 6. XRD of Cs-tungstates synthesized from amorphous Cs-IPA in a reducing atmosphere. (a) Cs/W = 0.30, heat-treated in 10% H_2/0.5% H_2O/N_2-balance at 600°C for 1 hr; (b) Cs/W = 0.48, in 10% H_2/0.5% H_2O/N_2-balance at 600°C for 1 hr; (c) Cs/W = 0.48, in H_2/H_2O at 700°C for 1 hr.

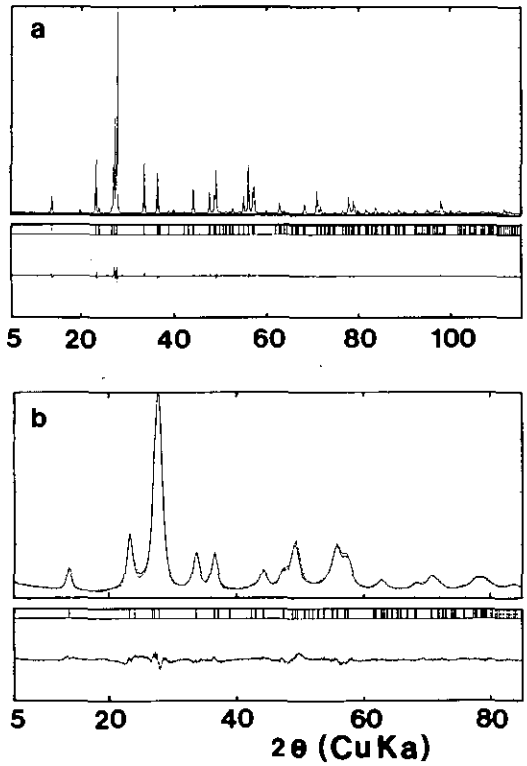

FIG. 7. The observed and calculated powder XRD profiles for Cs-tungstates derived from Cs-IPA (Cs/W = 0.3). (a) Hex(red); heat-treated in 10% H_2/0.5% H_2O/N_2-balance (Cs_xWO_3, reduced phase); and (b) Hex(ox); in air ($CsyW_{1-y/6}O_3$, oxidized phase).

most an idealized form: The position of O(1) can be reduced from the 12*k* to the special 6*f* site within the error limit and the deviation of O(2) from its ideal position, 12*j*(x, y, $\frac{1}{4}$) where $x = 2y$ with $y = 0.211$, is less than 1%. Very near lattice parameters (a = 7.116(3), c = 7.5981(5)) and atomic positions have been reported by Kihlborg *et al.* for $Cs_{0.32}WO_3$ prepared from a mixture of Cs_2WO_4, WO_2, and WO_3 at 750°C in a sealed tube, through the R factors of their result ($R_f = 0.05$) are not so small as ours (*11*). Therefore, these two Cs-HTBs may be basically identical except for a slight difference in the Cs contents.

The structure of oxidized sample ($Cs_xWO_{3+x/2}$: $x = 0.30$) was also refined in the same space group and atomic distribution. In this case, however, an incomplete h-WO_3 type framework with W-defects was assumed, for there were no possible interstices for excess oxygens to be accommodated. As the compound is thus represented by $Cs_yW_{1-y/6}O_3$ where $y = 6x/(6 + x)$, the occupancy factors of the Cs, W, O(1), and O(2) sites were fixed at 0.857, 0.952, 0.5, and 1.0. The refined atomic parameters were five positional ones and the B-values of Cs and W ions. The oxygens B-values were fixed because they became negative due to correlation with other parameters, which happened frequently in powder refinement.

As shown in Fig. 7b, the observed and calculated patterns show good agreement ($R_{wp} = 0.07$, $R_f = 0.007$), though the profiles are rather broad. Crystallographic parameters after refinement is tabulated in Table IIb. As a whole, structural difference between the reduced and oxidized sample is not drastic, but the latter's c-axis is significantly elongated and the WO_6 octahedron is more distorted. It is also noted that the displacement of O(1) at 12*k* (x, 0, z) from the basal plane ($z = 0$) is considerably large ($z = 0.037(38)$), whereas reported z-values for various reduced HTBs are very close to zero. This generates a great deal of difference in the distances between W and two possible O(1) positions (1.71 and 2.15 Å). The shorter distance is comparable with that of W=O.

For pyrochlore-phase compounds, the rather poor crystallinity of the oxidized samples and contamination by impurity phases in the reduced samples have not permitted us to obtain a definitive structural determination. However, tentative analysis suggested that oxidized pyrochlore, represented by $Cs_yW_{1-y/6}O_3$ (z = I6), where $y = 6x/(6 + x)$, were substantially identical with our previously reported Cs-tungstate (*1*). Its cubic lattice parameter was 10.2555(14) Å for $x = 0.48$, and the reduced compound Cs_xWO_3 (with the same Cs/W ratio) showed a longer parameter, 10.3196(1)Å.

TABLE IIa

CRYSTALLOGRAPHIC DATA FOR Cs_xWO_3 OBTAINED AT 600°C IN A REDUCING ATMOSPHERE (x = 0.30 FROM CHEMICAL ANALYSIS)

System		Hexagonal; $P6_3/mcm$		
Space group		6		
Z		7.4049(1)		
a		7.6098(1)		
c				
Atomic position				
Atom	Site	Parameter	Occupancy	B
W	6g(x, 0, ¼)	x: 0.4857(3)	1.0	1.14(12)
O(1)	12k(x, 0, z)	x: 0.493(19)	0.5	0.59(5)
		z: 0.01(1)		
O(2)	12j(x, y, ¼)	x: 0.2102(29)	1.0	0.28(84)
		y: 0.4185(20)		
Cs	2b(0, 0, 0)		0.9	0.86(44)

Interatomic distance (Å)			
W–O in WO_6 octahedron		O(2)–O(2) in hexagonal tunnel	
W–O(1)	1.84	O(2)–O(2)	2.67
	1.84		2.70
W–O(2)	2.01	O(2)–O(2) in prism tunnel	
	2.01	O(2)–O(2)	2.76
	1.83		
	1.98	O(2)–O(1) in octahedron	
		O(2)–O(1)	2.62
Cs–O(2)	3.29		2.73
	4.52		2.63
			2.79

Note. R_f = 0.024.

Structural Change on Redox Reaction

A pale-yellow oxidized form of hexagonal $Cs_yW_{1-y/6}O_3$ ($y = 6x/(6 + x)$: $x = 0.30$), prepared by heating Cs-IPA in air at 600°C, was changed into a dark-blue reduced form by reduction in a reducing atmosphere (10% H_2/0.5% H_2O/N_2-balance) at the same temperature. As shown in Fig. 8a, its XRD pattern exactly agrees with Fig. 6a recorded with the sample obtained by heating Cs-IPA in the same reduction atmosphere at 600°C, indicating that these two reduced compounds are identical. Reoxidizing them in air at the same temperature yielded a pale yellow hexagonal phase (Fig. 8b), which is substantially similar to the initial oxidized form except for a considerable difference in their crystallinity and lattice parameters (reoxidized compound: a = 7.373 and c = 7.717 Å). For further redox repetition, however, the reaction in the hexagonal phases (denoted "Hex"),

$$\text{Hex(ox)} \leftrightarrow \text{Hex(red)} \qquad (1)$$

was perfectly reversible, including those crystallographic points.

Infrared spectra recorded with Hex(ox) and Hex(red) using the KBr pellet technique are shown in Fig. 9. A very sharp band at 950 cm^{-1} seen in the former's spectrum (Fig. 9a) may be assigned to W = O (terminal), indicating that part of W are vacant in the Hex(ox) framework. However, this band is almost missing in the latter's spectrum (Fig. 9b). Therefore, the compounds may be formulated as Hex(ox): $Cs_yW_{1-y/6}O_3$ (y =

TABLE IIb

CRYSTALLOGRAPHIC DATA FOR $Cs_xW_{1-x/6}O_3$ OBTAINED AT 600°C IN AIR (x = 0.29 FROM CHEMICAL ANALYSIS)

System				
Space group		Hexagonal; $P6_3/mcm$		
Z		6		
a		7.4012(18)		
c		7.6728(17)		
Atomic position				
Atom	Site	Parameter	Occupancy	B
W	6g(x, 0, ¼)	x: 0.4927(7)	0.95	1.31(7)
O(1)	12k(x, 0, z)	x: 0.5242(73)	0.5	1.3
		z: 0.037(38)		
O(2)	12j(x, y, ¼)	x: 0.2086(73)	1.0	1.3
		y: 0.4270(13)		
Cs	2b(0, 0, 0)		0.86	2.40(15)

Interatomic distance (Å)			
W–O in WO_6 octahedron		O(2)–O(2) in hexagonal tunnel	
W–O(1)	2.15	O(2)–O(2)	2.79
	1.71		2.68
W–O(2)	1.90	O(2)–O(2) in prism tunnel	
	1.90	O(2)–O(2)	2.66
	1.98		
	1.98	O(2)–O(1) in octahedron	
		O(2)–O(1)	2.48
Cs–O(2)	3.34		2.98
	4.62		2.62
			2.78

Note. R_f = 0.007.

$6x/(6 + x)$) and Hex(red): Cs_xWO_3. It was shown by an *in situ* measurement that the weight change during reoxidizing process (+0.85%) agreed with the calculated value (+0.88%) within the experimental error limit. The densities of Hex(ox) and Hex(red) were 6.86 and 7.47 g · cm^{-3}, respectively, which are in principle in good agreement with their calculated value for six formula units per cell, 7.17 and 7.50 g · cm^{-3}. A slight discrepancy (~4%) in Hex(ox) can be accounted for by either the measurement error due to closed micropores in the sample or incorporation of oxygen vacancies in the anion sublattice, which has been proposed by Driouiche *et al.* (*4*) for their pyrochlore-type Cs(or Rb)-tungstate.

Similar redox experiments were also performed with Cs-tungstate (Cs/W = 0.48) in the pyrochlore form. Initial oxidized compound (Pyro(ox)) obtained by heating Cs-IPA in air at 600°C turned into a reduced pyrochlore form (Pyro(red)) after treatment in a reducing atmosphere (H_2/H_2O) at 700°C, which was identical with the compound previously shown in Fig. 6c as their cell parameters agreed with each other. As shown in Fig. 9d, Pyro(red) shows no band at around 950 cm^{-1}, which is clearly seen in the spectrum of Pyro(ox) as shown in Fig. 9c. Thus, the former is likely to be based on a complete pyrochlore framework (i.e., Cs_xWO_3), while the latter on a lacunar one ($Cs_yW_{1-y/6}O_3$ where $y = 6x/(6 + x)$), as pointed out by the present authors (*2*) and Driouiche *et al.* (*4*) for their Cs-tungstates in an oxidized form.

Reoxidation of Pyro(red) resulted in a

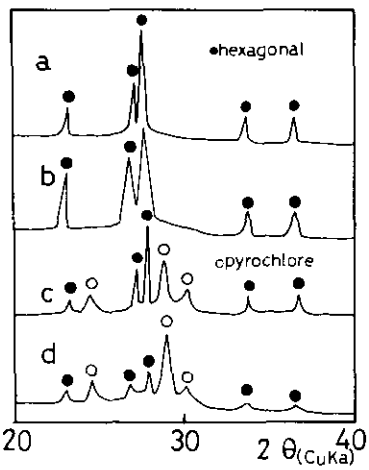

FIG. 8. The change of XRD of Cs-tungstates on the redox reaction. Hex(ox), Cs/W = 0.30, heat-treated in air at 600°C. Hex(red), Cs/W = 0.30, in 10% H_2/0.5% H_2O/N_2-balance at 600°C. Pyro(red), Cs/W = 0.48, in H_2/H_2O at 700°C. (a) heat-treated Hex(ox) in 10% H_2/0.5% H_2O/N_2-balance at 600°C for 1 hr; (b) heat-treated Hex(red) in air at 600°C for 1 hr; (c) heat-treated Pyro(red) in air at 600°C for 1 hr; and (d) heat-treated Pyro(red) in air at 600°C for 8 hr.

mixture of pyrochlore and hexagonal phase, as shown in Fig. 8c, and Pyro(ox) in a pure phase could not be obtained even after treatment for 8h at 600°C, as shown in Fig. 8d. At higher temperature, additional peaks of unknown phase appeared in the XRD pattern. Consequently, the redox reaction in the pyrochlore phase is virtually irreversible.

In addition, it is interesting to discuss the schemes of those reactions. As mentioned above, reduction of Pyro(ox) at 600°C (or lower) gives a mixture of a pyrochlore and hexagonal phase. To follow this process, XRD patterns were taken with some samples treated for various times at 600°C in an H_2/H_2O atmosphere. As shown in Fig. 10a, the sample at initial 1 hr consists of a reduced hexagonal (a = 7.40, c = 7.61 Å) and a pyrochlore phase left almost not reduced (a = 10.27 Å). It is, therefore, suggested that the initial stage of reduction is disproportion of Pyro(ox) according to

$$Cs_yW_{1-y/6}O_3 \rightarrow a_1Cs_{1/3}WO_3 + a_2Cs_{1/2}W_{11/12}O_3, \quad (2)$$

where $y = 6x/(6 + x) = 0.44$, if full occupancy of the Cs sites ($2b$ in hex. and $8b$ in pyro.) and a complete anion sublattice are assumed in both resultant compounds. This assumption requires that the fraction $a_1/(a_1 + a_2)$ must be less than about 0.3. This value could be larger, if the Cs/W ratio in the pyrochlore phase is permitted to be larger than 6/11. As the reaction time is prolonged, peaks due to the hexagonal phase become weaker, and very sharp ones assigned to reduced pyrochlore (a = 10.32 Å) are strengthened instead, as shown in Fig. 10b. These results indicate that Pyro(red) is formed by solid-state reaction between the products of reaction (2),

$$a_1Cs_{1/3}WO_3 + a_2Cs_{1/2}W_{11/12}O_3 \rightarrow Cs_xWO_3(\text{pyro}), \quad (3)$$

which may be remarkably slower than the preceding disproportionation Eq. (2). Even after prolonged treatment for 10 hr at 600°C,

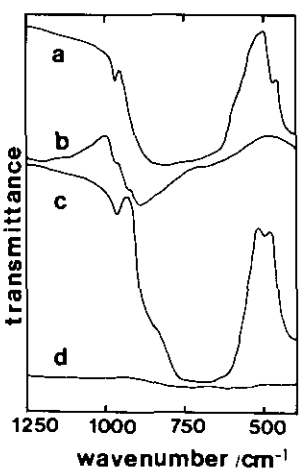

FIG. 9. IR spectra of Cs-tungstates synthesized from Cs-IPA. (a) Hex(ox); Cs/W = 0.30, heat-treated in air at 600°C for 1 hr; (b) Hex(red); Cs/W = 0.30, in 10% H_2/0.5% H_2O/N_2-balance at 600°C; (c) Pyro(ox); Cs/W = 0.48, in air at 600°C; and (d) Pyro(red); Cs/W = 0.48, in H_2/H_2O at 700°C.

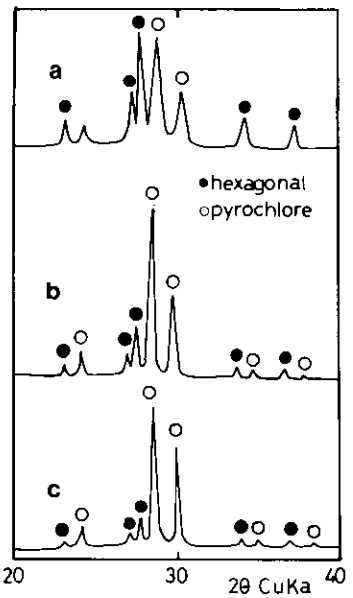

FIG. 10. XRD of Cs-tungstates synthesized from pyrochlore-oxidized form heat-treated in H_2/H_2O at 600°C for different heating times. (a) 1 hr, (b) 5 hr, and (c) 10 hr.

hexagonal peaks are still observable, as shown in Fig. 10c.

Reoxidation of Pyro(red) as shown in Figs. 8c and 8d seems to proceed in the same way but in a reverse manner. In this case, however, formation of the defective pyrochlore framework according to the reversal of Eq. (2) may be very slow.

Such reaction paths as in the above are not surprising, because the structure of hexagonal and pyrochlore frameworks are closely related to each other. As previously pointed out by the present authors (*2*), there are two kinds of hexagonal frameworks: a normal h-WO_3-type ($P6_3/mcm$) (as is the case with the present hexagonal phase) and a type to be termed 2-D pyrochlore ($P6_3/mcm$). The latter type has recently been found in a kind of Ba- and Pb-tungstate (*1*, *2*) derived from peroxopolytungstate, in which layers formed out of six-membered rings of WO_6 octahedra, the same ones found in the (111) plane of the pyrochlore-type framework, are stacked in upside-down manner alternately by sharing their top and bottom apices, as shown in Fig. 11. The pyrochlore framework can be built up by inserting a WO_6 octahedron on the top oxygens around position A and then stacking the same six-membered ring layer with a translation of $(\frac{2}{3}, \frac{1}{3})$. It is, therefore, thought that the hexagonal phase (in a normal h-WO_3 type) produced during the redox process of pyrochlore-type Cs-tungstate is formed via such a 2-D pyrochlore framework.

The difference in the redox reversibility between pyrochlore and hexagonal structures might be attributed to whether their six-membered ring network is rigid 3-D or more loose 2-D. It is interesting to note that, if every seventh W layer of hexagonal $Cs_{1/3}WO_{3+1/6}$ is vacant, the compound would take a lamellar structure, represented as $Cs^+[Cs_5W_{18}O_{57}]^-$. Though such a superstructure was not observed in its powder XRD pattern, the oxygen transport needed for the redox process of the hexagonal phases seems to occur utilizing interlayer regions of the lamellar structure partly generated in the compound.

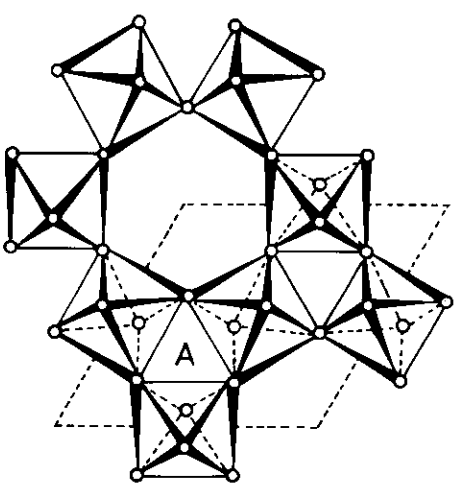

FIG. 11. Idealized expression of the 2D-pyrochlore type-WO_3 framework (projection along the [001] axis).

Conclusions

We synthesized two kinds of cesium-tungstates through thermal decomposition of cesium peroxo-polytungstate as a precursor at relatively low temperature. Cesium-rich precursors ($Cs/W \geq 0.48$) gave tungstates with a pyrochlore-type framework, similar to the compound that Driouiche *et al.* had synthesized from h-WO_3 and cesium carbonate. A precursor with a low cesium content ($Cs/W \approx 0.30$) yielded a compound based on an h-WO_3-type framework with tungsten vacancies. This is the first synthesis of a fully oxidized cesium-tungstate in a hexagonal form, though hexagonal Cs-HTBs have long been known. On reduction, it turned into a hexagonal compound substantially similar to Cs-HTB, which could reversibly be reoxidized into its initial form. The pyrochlore phase was also reduced to form a compound based on the same type of framework in a reduced form. However, this process was not topochemical but proceeded via formation of a hexagonal phase. Reoxidation of the reduced pyrochlore compound resulted in a mixture of a pyrochlore and hexagonal phase. Such a redox behavior of the pyrochlore-type cesium-tungstate might be a reflection of structural similarity between the pyrochlore and the h-WO_3 framework. Further investigations are now in progress.

Acknowledgment

This work was partially supported by a Grant-in-Aid for Scientific Research from the Japanese Minister of Education, Science, and Culture (04205024).

References

1. T. Kudo, A. Kishimoto, and J. Oi, *Solid State Ionics* **40/41,** 567 (1990).
2. T. Kudo, J. Oi, and A. Kishimoto, *Mater. Res. Bull.* **26,** 779 (1991).
3. A. Coucou and M. Figlarz, *Solid State Ionics* **28–30,** 1762 (1988).
4. A. Driouiche, F. Abraham, M. Touboul, and M. Figlarz, *Mater. Res. Bull.* **26,** 901 (1991).
5. Kenneth P. Reus, A. Ramanan, and M. Stanley Whittingham, *J. Solid State Chem.* **96,** 31 (1992).
6. A. Magneli and B. Blomberg, *Acta Chem. Scand.* **5,** 372 (1951).
7. T. Kudo, H. Okamoto, K. Matsumoto, and Y. Sasaki, *Inorg. Chim. Acta* **27,** 111 (1986).
8. T. Nanba, S. Takano, I. Yasui, and T. Kudo, *J. Solid State Chem.* **90,** 47 (1991).
9. F. Izumi, *Nippon Kessho Gakkaishi* **27,** 23 (1985).
10. M. F. Pye and P. G. Dickens, *Mater. Res. Bull.* **14,** 1397 (1979).
11. L. Kihlborg and A. Hussain, *Mater. Res. Bull.* **14,** 667 (1979).
12. P. P. Labbe, M. Goreaud, B. Raveau and J. C. Monier, *Acta Crystallogr. Sect. B* **34,** 1433 (1978).